



## Study of the adsorption of Co(II) on the chitosan-hydroxyapatite

Zhiguang Ma \*, Mengchao Liu, Jianghong Li, Yinan Song and Suwen Liu

College of Chemistry and Environmental Science, Key Laboratory of Medicinal Chemistry and Molecular Diagnosis, Hebei University, Baoding 071002, China

\*Corresponding author at: College of Chemistry and Environmental Science, Key Laboratory of Medicinal Chemistry and Molecular Diagnosis, Hebei University, Baoding 071002, China.

Tel.: +86.0312.5079359. Fax: +86.0312.5079525. E-mail address: [hymzq@163.com](mailto:hymzq@163.com) (Z. Ma).

### ARTICLE INFORMATION



DOI: 10.5155/eurjchem.5.2.209-213.948

Received: 18 October 2013

Received in revised form: 13 December 2013

Accepted: 16 December 2013

Online: 30 June 2014

### KEYWORDS

Cobalt  
Kinetics  
Chitosan  
Adsorption  
Hydroxyapatite  
Thermodynamics

### ABSTRACT

The adsorption of cobalt ions ( $\text{Co}^{2+}$ ) from aqueous solution onto chitosan-hydroxyapatite composite is investigated in this study. The effects of adsorption time, initial concentration, temperature, and pH are studied in details. Kinetics and thermodynamics of the adsorption of  $\text{Co}^{2+}$  onto the chitosan-hydroxyapatite are also investigated and the adsorption kinetics is found to follow the pseudo-second-order model with an activation energy ( $E_a$ ) of 10.73 kJ/mol. Thermodynamic studies indicates that the adsorption follows the Langmuir adsorption equation. The value of entropy change ( $\Delta S^\circ$ ) and enthalpy change ( $\Delta H^\circ$ ) are found to be 83.50 and 18.09 kJ/mol, respectively. The Gibbs free energy change ( $\Delta G^\circ$ ) is found to be negative at all five temperatures, demonstrating that the adsorption process is spontaneous and endothermic.

### 1. Introduction

In the earth's crust, the cobalt content is very high. Cobalt is very useful cemented carbide industry, ceramics, electroplating industry, and so on. Cobalt ion is toxic. Accumulated cobalt ion in human body can have serious effect on human health, resulting in dysfunctions of heart, lung, liver, spleen, stomach and other organs, and even causing cancers [1-3]. Therefore, many types of adsorption materials have been developed to remove  $\text{Co}^{2+}$  from aqueous solution. These materials include vermiculite [4], zeolite [5], sepiolite [6], kaolinite [7], and Chitosan-aluminium oxide [8]. In addition, the Chitosan-aluminium oxide material was also used to remove  $\text{Zn}^{2+}$  from aqueous solution [9].

Chitosan (CS) can be obtained through deacetylation of the natural polymer chitin which widely exists in nature. There is a large number of hydroxyl and amino groups in the chitosan chain, which can be used as adsorbent for the heavy metal ions in wastewater [10-14]. However, as an adsorbent, the mechanical strength of chitosan is not very good, and its dissolution in the acidic solution can also have negative effect on its performance. Hydroxyapatite (HA) has unique chemical structure and is widely used to adsorb metal ions [15]. So, chitosan-hydroxyapatite (CS/HA) composite material is expected to be able to overcome the shortcoming of chitosan. For example, a CS/HA composite material has been prepared

by Xie *et al.* using chitosan, lime nitrate tetra-hydrate, and potassium di-hydrogen phosphate [16].

In this manuscript, we focus on a better understanding of the fundamental aspects of the adsorption of heavy metal such as cobalt onto CS/HA composite material and present a thorough kinetic and thermodynamic investigation of the adsorption process. We hope our studies can provide valuable insights for a better design of chitosan-inorganic composite materials.

### 2. Experimental

#### 2.1. Materials

Chitosan (>90%) is purchased from Zhejiang Golden-Shell Biochemical Co., Ltd., China. Cobalt nitrate ( $\text{Co}(\text{NO}_3)_2 \cdot 6\text{H}_2\text{O}$ ) (>99.5%) is purchased by Sinopharm Chemical Reagent Co., Ltd. China. Acetic acid, calcium nitrate ( $\text{Ca}(\text{NO}_3)_2 \cdot 4\text{H}_2\text{O}$ ), potassium dihydrogen phosphate ( $\text{KH}_2\text{PO}_4$ ), hydrochloric acid (HCl), and sodium hydroxide (NaOH) are of analytical reagent grade and were purchased from Tianjin Chemical Reagent Co., Ltd, China. All solutions are prepared in deionized water. Hydrochloric acid and NaOH are used to adjust the pH.

#### 2.2. Preparation of CS/HA

CS/HA composite material is prepared according to the procedure described in previous study [16]. Briefly, 100 g of chitosan is added into 75 mL of 2% acetic acid, and then 1.25 g of  $\text{Ca}(\text{NO}_3)_2 \cdot 4\text{H}_2\text{O}$  and 0.43 g of  $\text{KH}_2\text{PO}_4$  were added into the solution. The combination of  $\text{Ca}(\text{NO}_3)_2 \cdot 4\text{H}_2\text{O}$  and  $\text{KH}_2\text{PO}_4$  results in the formation of hydroxyapatite (HA) in situ. The relative ratio of CS over HA is kept at 10:1. During the preparation, about 3-8% NaOH solution should be added to the mixture under stirring to give an uniform and transparent solution. After the reaction is completed, it is allowed to stand for 12 h. The crude product is washed until the pH is neutral, and then dried at 338 K in the oven. The final product is then ground to 80 mesh.

### 2.3. Methods

All batch adsorption experiments are conducted in 50 mL flask. A mixture of 0.5 g of adsorbents and 25 mL of  $\text{Co}(\text{NO}_3)_2$  solution of different initial concentration is added into the flask. The hydrochloric acid solution and sodium hydroxide solution are used to adjust the pH. The flask is shaken in a thermostated shaker at 130 rpm under different temperatures. After adsorption, the adsorbent is filtered and the concentration of the  $\text{Co}^{2+}$  in the filtrate is determined by UV-Vis spectroscopy using 512 nm. Adsorption capacity is calculated according to Equation 1.

$$Q = (C_0 - C) \times V / m \quad (1)$$

where  $Q$  (mmol/g) is adsorption capacity,  $C_0$  (mol/L) and  $C$  (mol/L) are the initial concentration and the final concentration of  $\text{Co}^{2+}$ ,  $V$  (mL) is the solution volume, and  $m$  (g) is the adsorbent mass.

## 3. Results and discussion

### 3.1. Influence of adsorption time on the adsorption capacity

We first determined the optimum adsorption time. We studied the influence of adsorption time on the adsorption capacity at 298.2 K with an initial  $\text{Co}^{2+}$  concentration of 0.1000 mol/L. As we can see in Figure 1, the adsorption capacity reaches a plateau after 480 min adsorption. This adsorption time is then used as the optimum adsorption time in the following experiments.

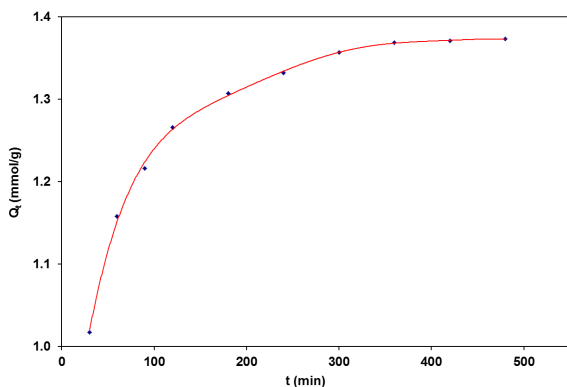


Figure 1. The influence of time on the adsorption capacity of  $\text{Co}^{2+}$ .

### 3.2. Influence of temperature on the adsorption capacity

We then studied the influence of temperature on adsorption capacity. At five different temperatures of 293.2, 298.2, 308.2, 318.2, and 328.2 K, the influence of adsorption temperature is investigated with the  $\text{Co}^{2+}$  concentration of 0.1000 mol/L. The results illustrate in Figure 2 shows that with

the increase of temperature, the adsorption capacity increases rapidly. Based on this result, we can infer that the adsorption is an endothermic process.

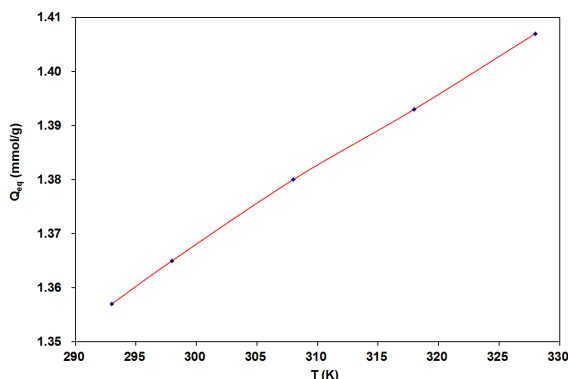


Figure 2. The influence of temperature on the adsorption capacity of  $\text{Co}^{2+}$ .

### 3.3. Influence of initial $\text{Co}^{2+}$ concentration on the adsorption capacity

The influence of initial concentration on adsorption capacity is studied at 298.2 K with the adsorption time of 480 minute. As shown in Figure 3, it is found that the adsorption capacity varies with the initial concentration of  $\text{Co}^{2+}$ . The results illustrate that the adsorption capacity of  $\text{Co}^{2+}$  on the CS/HA increases with the initial concentration increasing. The adsorption capacity grows rapidly when initial concentration is smaller than 0.2500 mol/L, and then trends to slow down when the initial concentration is 0.2500 mol/L capacity. This may be caused by an increase in the driving force of the concentration gradient with the increase in the initial concentration [17].

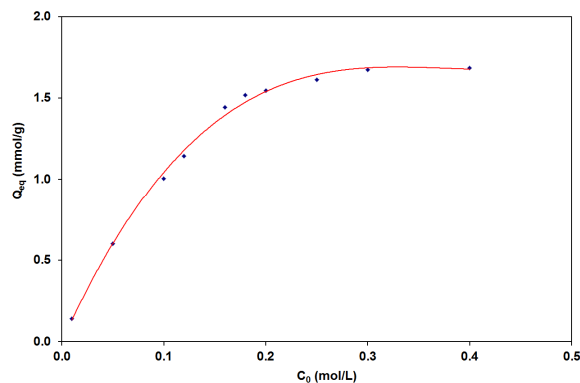


Figure 3. The influence of the initial concentration on the adsorption capacity of  $\text{Co}^{2+}$ .

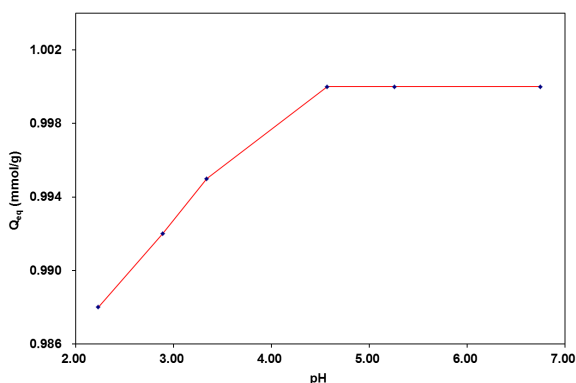
### 3.4. Influence of pH on the adsorption capacity

As is well known, the pH of solution is an important parameter affecting the adsorption of metal ions on the adsorbents as it not only influences metal speciation in solution, but also influences the surface properties of the adsorbents due to the dissociation of functional groups and the variation of surface charges under different pHs [18]. In order to evaluate the influence of pH on the adsorption of  $\text{Co}^{2+}$ , the effect of pH on the adsorption capacity is studied. The experiment is conducted in the pH range from 2.2 to 6.8, and the influence of pH on the adsorption capacity is thus determined. Results in Figure 4 illustrate that pH has little effect on the adsorption capacity when pH increases from 2.2 to 4.6 and then reaches a plateau at pH = 6.8.

**Table 1.** Fitting results of the pseudo-second-order equation

T (K)	Fitting equation	Q <sub>eq</sub> (mmol/g)	k (g/mmol·min)	r <sup>2</sup>
293	t/Q <sub>t</sub> = 0.7114t + 10.66	1.406	0.04747	0.9999
298	t/Q <sub>t</sub> = 0.7071t + 9.590	1.412	0.05409	0.9999
308	t/Q <sub>t</sub> = 0.7051t + 8.162	1.418	0.06227	0.9999
318	t/Q <sub>t</sub> = 0.7035t + 6.553	1.434	0.06793	0.9999
328	t/Q <sub>t</sub> = 0.6969t + 5.587	1.454	0.07692	0.9999

In addition, at pH = 6.8 the solution becomes turbid and some precipitates become visible. At low pH, more protons will be available to protonate the amine groups in chitosan [19], thus reducing the number of binding sites for the adsorption of Co<sup>2+</sup>. This is why we observe a low adsorption capacity at low pH. So, we can conclude that the optimum pH for Co<sup>2+</sup> adsorption is between 5 and 7. In a previous study, the presence of cobalt ionic speciation was investigated and the results showed that cobalt is present in the aqueous solution mainly in the form of Co<sup>2+</sup> up to pH = 8. This means that in the initial pH range of 4-8, cobalt ion is adsorbed on the adsorbent through an ion exchange process with hydroxyapatite [20].

**Figure 4.** The influence of pH on adsorption capacity of Co<sup>2+</sup>.

### 3.5. Kinetic studies on the adsorption of Co<sup>2+</sup> on the CS/HA

The adsorption kinetic curves of the 0.1000 mol/L Co<sup>2+</sup> on the CS/HA composite material at different temperatures are studied. At the early stage, the adsorption rate is fast, and then decreases with time. After about 420 minutes, the adsorption reaches equilibrium, as shown in Figure 5. At the beginning, the adsorption of Co<sup>2+</sup> mainly occurs on the external surface of CS/HA and the adsorption rate thus increases rapidly. In the second stage, as the adsorbed cobalt ions diffuses inward into the CS/HA through the micropore, the resistance of diffusion increases with adsorption procedure. Adsorption rate is mainly controlled by diffusion at this stage, so the rate of adsorption becomes small. At the final stage, the adsorption mainly occurs on the inner surface of adsorbent and the adsorption reaches equilibrium. So, this adsorption procedure is generally consistent with a three-step adsorption behavior which is usually observed from porous adsorbents [21,22].

Pseudo-second-order kinetics model is based on the assumption of that: the rate of adsorption is determined by the square of the number of vacancies [23]. The formula is:

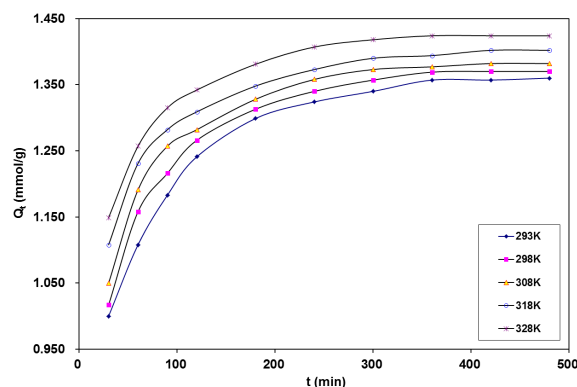
$$dQ_t/dt = k(Q_{eq} - Q_t)^2 \quad (2)$$

Integration of the Equation 2 under boundary conditions leads to Equation 3.

$$t/Q_t = t/Q_{eq} + 1/kQ_{eq}^2 \quad (3)$$

where Q<sub>t</sub> (mmol/g) is the absorption capacity at any time; and Q<sub>eq</sub> (mmol/g) is the absorption capacity at equilibrium; k (g/mmol·min) is the adsorption rate constant.

If adsorption procedure conforms to the pseudo-second-order equation, t/Q<sub>t</sub> and t could have a linear relationship. Indeed, fitting the data in Table 1 shows that the pseudo-second-order kinetic model has a good correlation coefficient (r<sup>2</sup> = 0.9999), indicating that the kinetic model fits well with the experimental data. The pseudo-second-order model supports that the rate-limiting step may be sorption involving valency forces through sharing or exchange of electrons between the -NH<sub>2</sub> groups in chitosan and Co<sup>2+</sup> [24,25].

**Figure 5.** Adsorption kinetic curves at different temperatures.

Temperature study (Figure 6) shows a r<sup>2</sup> value of 0.99. This indicates that the relationship between temperature and the rate of absorption obeys the Arrhenius equation:

$$\ln k = -E_a/RT + \ln A \quad (4)$$

The temperature has significant effects on the rate constant k. According to the Arrhenius equation, the obtained E<sub>a</sub> is 10.73 kJ/mol.

### 3.6. Thermodynamic studies on the adsorption of Co(II) on the CS/HA

The adsorption thermodynamic curve of Co<sup>2+</sup> concentrate on the CS/HA at different temperatures is detected using the absorption time of 480 minute. Results illustrate that the adsorption capacity of Co<sup>2+</sup> on the CS/HA increases with the increase of the initial concentration of Co<sup>2+</sup>, and then it reaches a maximum value (Figure 7). This is due to that the amount of CS/HA is at a fixed value and thus the number of adsorption sites is at a fixed value too [26]. At the beginning of the adsorption, the CS/HA could provide enough sites, thus the adsorption capacity of CS/HA is high; however, the active sites become insufficient when the initial concentration of Co<sup>2+</sup> is high and the adsorption sites could be saturated under such situation.

The expression of the Langmuir adsorption model [27] is listed as below.

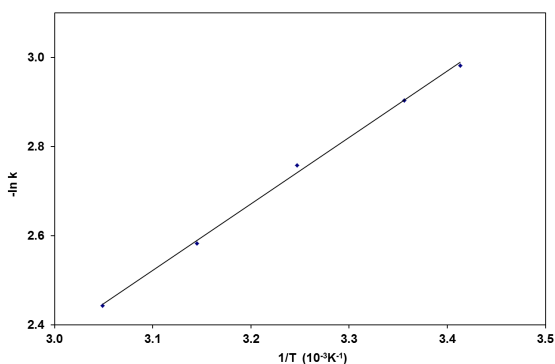
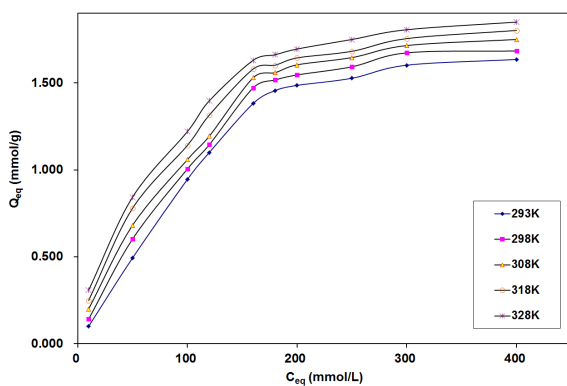
$$C_{eq}/Q_{eq} = C_{eq}/Q_m + 1/K_L Q_m \quad (5)$$

**Table 2.** Parameters and equations for Langmuir adsorption model at five different temperatures

T (K)	Langmuir equation	$Q_m$ (mmol/g)	$K_L$ (L/mmol)	$r^2$
293	$C_{eq}/Q_{eq}=0.5063C_{eq}+35.55$	1.975	0.01424	0.9955
298	$C_{eq}/Q_{eq}=0.4940C_{eq}+31.52$	2.024	0.01567	0.9958
308	$C_{eq}/Q_{eq}=0.4910C_{eq}+25.86$	2.037	0.01899	0.9972
318	$C_{eq}/Q_{eq}=0.4892C_{eq}+19.43$	2.044	0.02517	0.9968
328	$C_{eq}/Q_{eq}=0.4870C_{eq}+16.02$	2.053	0.03040	0.9978

**Table 3.** Thermodynamic parameters at different temperatures

T (K)	$\Delta G^\circ$ (kJ/mol)	$\Delta H^\circ$ (kJ/mol)	$\Delta S^\circ$ (J/mol·K)	$r^2$
293.2K	-6.376	18.09	83.50	0.9888
298.2K	-6.793			
308.2K	-7.628			
318.2K	-8.463			
328.2K	-9.298			

**Figure 6.** Relationship between  $-\ln k$  and  $1/T$ .**Figure 7.** Adsorption capacity of  $Co^{2+}$  at different temperatures.

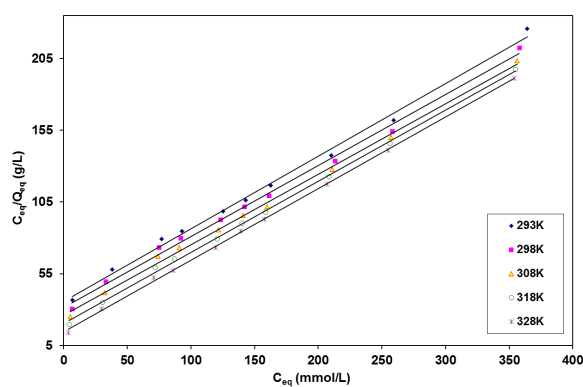
where  $C_{eq}$  and  $Q_{eq}$  are the equilibrium concentration of metal ions (mmol/L) and the adsorption capacity (mmol/g), respectively;  $Q_m$  is adsorption capacity (mmol/g);  $K_L$  is the equilibrium constant (L/mmol).

The experiment data (Figure 8) are fitted using Langmuir equation and the corresponding adsorption parameters along with regression coefficients are listed (Table 2). From Figure 8, we can see that the adsorption of  $Co^{2+}$  onto the CS/HA can be fitted well according to the Langmuir model. Langmuir model assumes that the adsorbent surface has adsorption sites with identical energy and each adsorbed molecule takes part in a single site [28], thus following a monolayer adsorption model. From Table 2, we can see that the  $Q_m$  and  $K_L$  increase with increasing temperature. The result shows that the adsorption of  $Co^{2+}$  onto the CS/HA is an endothermic process.

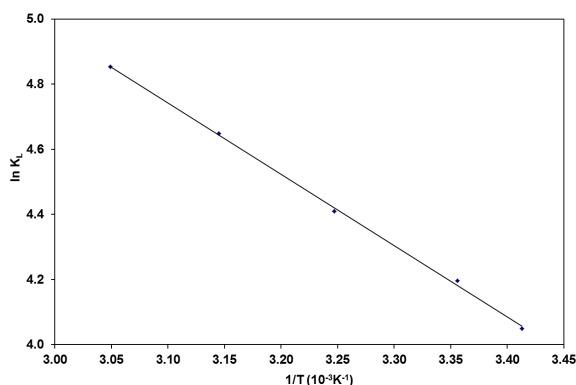
The relationship between  $K_L$  and  $T$  can be obtained from the Van't Hoff equation [29,30]. It is listed below.

$$\ln K_L = -\Delta H^\circ/RT + \Delta S^\circ/R \quad (6)$$

where  $\Delta H^\circ$  (J/mol) and  $\Delta S^\circ$  (J/mol·K) are the enthalpy and the entropy of the adsorption, respectively;  $R$  is the ideal gas constant;  $T$  (K) is temperature.

**Figure 8.** Relationship between  $C_{eq}/Q_{eq}$  and  $C_{eq}$ .

As is shown,  $\ln K_L$  has a linear relationship with  $1/T$  with an  $r^2$  value of 0.9888 (Figure 9). The slope and intercept are  $-\Delta H^\circ/R$  and  $\Delta S^\circ/R$ , respectively. And  $\Delta H^\circ$  and  $\Delta S^\circ$  are determined to be 18.09 kJ/mol and 83.50 J/mol·K, respectively. The results of  $\Delta G^\circ$  are listed in Table 3.

**Figure 9.** Relationship between  $\ln K_L$  and  $1/T$ .

The value of  $\Delta H^\circ$  is positive, which indicates that, the adsorption of  $Co^{2+}$  onto the CS/HA is an endothermic process. The value of  $\Delta S^\circ$  is positive, which also indicated that the process is caused by the increased randomness during the adsorption of  $Co^{2+}$  [16]. The value of  $\Delta G^\circ$  is negative at all of the five temperatures. The  $\Delta G^\circ$  decreases with the increase of temperature. It suggests that the adsorption of  $Co^{2+}$  onto the CS/HA is a spontaneous process. The spontaneous degree becomes greater with the increase of temperature. Therefore,

increasing temperature is beneficial to the adsorption procedure [31].

#### 4. Conclusion

The chitosan-hydroxyapatite composite material is prepared using chitosan, lime nitrate tetra-hydrate and potassium di-hydrogen phosphate as raw material by in situ composite method. The influences of adsorption time, temperature, initial cobalt concentration and pH on the adsorption kinetic and thermodynamic of  $\text{Co}^{2+}$  are studied. Our results show that the optimum time is 480 min and the optimum pH is between 5 and 7. The adsorption kinetics of  $\text{Co}^{2+}$  on the CS/HA is found to follow the pseudo-second-order kinetic model, and the apparent adsorption activation energy is measured to be 10.73 kJ/mol. The Langmuir adsorption model fits well with the experimental data. The adsorption thermodynamic parameters such as  $\Delta H^\circ$ ,  $\Delta S^\circ$ , and  $\Delta G^\circ$ , are obtained, which indicate that the adsorption process is spontaneous and endothermic.

#### Acknowledgements

This work was supported by the National Natural Science Foundation of China (Project No: 61001051), the Natural Science Foundation of Hebei Province (Project No: F2011201102).

#### References

- [1]. Ouyang, H. F. *J. Chin. Feed.* **1999**, *15*, 28-29.
- [2]. Li, Y. D.; Yuan, Z. H.; Li, H. Q. *J. Bull. Chin. Agric. Sci.* **2007**, *23*, 458-461.
- [3]. Huang, W. H.; Su, H. D. *Trans. Shenyang Ligong Univ.* **2008**, *27*, 87-90.
- [4]. Fonseca, M. G.; Oliveira, M. M.; Arakaki, L. N. H.; Espinola, J. G. P.; Airoldi, C. *J. Colloid Interf. Sci.* **2005**, *285*, 50-55.
- [5]. Erdem, E.; Karapinar, N.; Donat, R. *J. Colloid Interf. Sci.* **2004**, *280*, 309-314.
- [6]. Kara, M.; Yuzer, H.; Sabah, E.; Celik, M. S. *Water Res.* **2003**, *37*, 224-232.
- [7]. Yavuz, O.; Altunkaynak, Y.; Guzel, F. *Water Res.* **2003**, *37*, 948-952.
- [8]. Ma, Z. G.; Liu, S. W.; Zhang, H. L.; Liu, P.; Di, N. *Int. J. Chem.* **2011**, *3*, 116-120.
- [9]. Ma, Z. G.; Di, N.; Zhang, F.; Gu, P. P.; Liu, S. W.; Liu, P. *Int. J. Chem.* **2011**, *3*, 18-23.
- [10]. Li, Q.; Xi, D. L. *J. Environ. Prot. Chem. Ind.* **2005**, *25*, 350-352.
- [11]. Yang, M. P.; Li, G. B. *J. Mater. Prot.* **2003**, *36*, 37-38.
- [12]. Chu K. H. *J. Hazard. Mater.* **2002**, *90*, 77-95.
- [13]. Burke, A.; Yilmaz, E.; Hasirci, N. *J. Appl. Polym. Sci.* **2002**, *84*, 1185-1192.
- [14]. Dhakal, R. P.; Inoue, K.; Yoshizuka, K. *Solvent Extr. Ion Exc.* **2005**, *23*, 204-208.
- [15]. Liu, H. D.; Li, F. Z.; Zhao, X. *Chin. J. Process Eng.* **2008**, *8*, 42-47.
- [16]. Li, B. Q.; Hu, Q. L.; Wang, M.; Shen, J. C. *Chem. J. Chin. Univ.* **2004**, *10*, 1949-1952.
- [17]. Chiou, M. S.; Hsing, Y. L. *J. Hazard. Mater.* **2002**, *93*, 233-248.
- [18]. Qu, R. J.; Sun, C. M.; Wang, M. H. *Hydrometallurgy* **2009**, *100*, 65-71.
- [19]. Wan-Ngah, W. S.; Ghani, S. A.; Kamari, A. *Biores. Technol.* **2005**, *96*, 443-450.
- [20]. Smiciklas, I.; Dimovic, I.; Plecas, I.; Mitric, M. *Water Res.* **2006**, *40*, 2267-2274.
- [21]. Huang, Y. R.; Li, Z. J.; Wang, H. F.; Miao, Z. C.; Liu, J. G. *Appl. Chem.* **2009**, *38*, 1093-1097.
- [22]. Sun, X. L.; Zeng, Q. X.; Feng, C. G. *Acta. Phys. Chim. Sin.* **2009**, *25*, 1951-1957.
- [23]. Mohan, D.; Pittman, J. C. U. *J. Hazard. Mater.* **2006**, *137*, 762-811.
- [24]. Sag, Y.; Aktay, Y. *Biochem. Eng. J.* **2002**, *12*, 143-153.
- [25]. Wan-Ngah, W. S.; Ab-Ghani, S.; Kamari, A. *Bioresource Technol.* **2005**, *96*, 443-450.
- [26]. Huang, J. H. *J. The Light Text. Ind. Fujian.* **2005**, *7*, 15-17.
- [27]. Langmuir, I. *J. Am. Chem. Soc.* **1916**, *38*, 2221-2295.
- [28]. Vasconcelos, H. L.; Favere, V. T.; Goncalves, N. S.; Laranjeira, C. M. *React. Funct. Polym.* **2007**, *67*, 1052-1060.
- [29]. Atia A.; Donia A.M.; El-Boraey H.A. *Sep. Purif. Technol.* **2006**, *48*, 281-287.
- [30]. Ozcan, A.; Ozcan, A. S.; Tunali, S.; Akar, T.; Kiran, I. *J. Hazard. Mater.* **2005**, *124*, 200-208.
- [31]. Tang, J. Y.; Li, X.; Ying, H. J. *J. Nanjing Univ. Technol.* **2006**, *28*, 79-83.